Influence of subhumid climate and water table depth on groundwater recharge in shallow outwash aquifers

B. D. Smerdon,[1] C. A. Mendoza,[1] and K. J. Devito[2]

Received 15 August 2007; revised 16 May 2008; accepted 28 May 2008; published 22 August 2008.

[1] Hypothetical one-dimensional models of unsaturated flow were used to estimate the probability of groundwater recharge to shallow, glacial outwash aquifers. Simulations were supported by field data, previous three-dimensional modeling, and cross-sectional models of water table response to precipitation events for a research area in northern Alberta, Canada. Groundwater recharge rates were found to depend on the year-to-year climate variation, the depth to the water table, and were largely driven by annual snowmelt. Simulations indicate that in summer months, when transpiration and canopy interception were considered explicitly, groundwater recharge was negligible. For water table depths less than 6 m below ground surface, the occurrence of recharge depends on climatic conditions (water deficit or surplus) of the current and previous year, and can vary from 0 to 266 mm yr^{-1}. For water table depths of 6 m or more, recharge will depend on climate conditions from the most recent decade, have less annual variability, and a mean annual rate of approximately 45 mm yr^{-1}.

Citation: Smerdon, B. D., C. A. Mendoza, and K. J. Devito (2008), Influence of subhumid climate and water table depth on groundwater recharge in shallow outwash aquifers, *Water Resour. Res.*, *44*, W08427, doi:10.1029/2007WR005950.

1. Introduction

[2] Groundwater recharge is an essential hydrologic process, which generally describes the portion of water fluxes from the atmosphere that migrate to the groundwater regime. Recharge estimates are vital for developing conceptual models of water cycling, balancing watershed budgets, and simulating the movement of fluids and solutes in the subsurface [*de Vries and Simmers*, 2002]. For semiarid and subhumid regions, an intricate relationship between the atmosphere and the hydrosphere develops, where infiltrating water may be drawn up by vegetation (through evapotranspiration) or stored in the unsaturated zone under diminished potential for vertical drainage due to low relative permeability associated with dry soils. On coarse-textured landforms (e.g., glacial outwash), the timing of groundwater recharge controls the configuration of the water table [*Winter*, 1986], and long-term maintenance of lakes and wetlands [*Anderson and Munter*, 1981; *Smerdon et al.*, 2007].

[3] In this study, the influence of climate and water table depth on groundwater recharge was investigated with models of 1D infiltration to a shallow outwash aquifer. Motivation for this study originated with a need to understand and characterize the groundwater recharge process for coarse-textured landforms in the western boreal forest of Canada, and to develop indices of groundwater recharge that could be used in models of water cycling. Simulations were based on conceptual models developed from field study and a calibrated 3D lake-groundwater flow model of a glacial outwash site at the Utikuma Research Study Area (URSA), in northern Alberta, Canada [*Smerdon et al.*, 2005, 2007].

[4] The influence of year-to-year climate variability was investigated by simulating infiltration (i.e., unsaturated flow) driven by 71 years of historic data, and predicting water fluxes for various water table depths. The motivation was not to replicate prior subsurface conditions, but rather to use historic climate data to investigate transient moisture conditions and determine a range of expected groundwater recharge rates. Two-dimensional (cross-sectional) models of existing and historic conditions were used to examine the suitability of parameters and justify the lower-boundary condition for the 1D recharge models. In many models of infiltration and recharge, the lower boundary is implemented as a unit-gradient boundary condition that allows water to drain from the system [*Scanlon et al.*, 2002], and we sought to explore a fixed water table boundary condition as an alternative approach. Recharge rates predicted by the 1D models are summarized for different water table depths and in a cumulative probability distribution. These recharge rates can be incorporated into regional hydrologic models and in predictive modeling to support large-scale reclamation projects and management programs (e.g., following open pit mining, forest harvest, or to assess the effect of forest fire). The methodology described in this study is similar to that used by *Keese et al.* [2005] to investigate diffuse groundwater recharge, and is suitable for simulating the response of landscapes

[1]Department of Earth and Atmospheric Sciences, University of Alberta, Edmonton, Alberta, Canada.
[2]Department of Biological Sciences, University of Alberta, Edmonton, Alberta, Canada.

0043-1397/08/2007WR005950

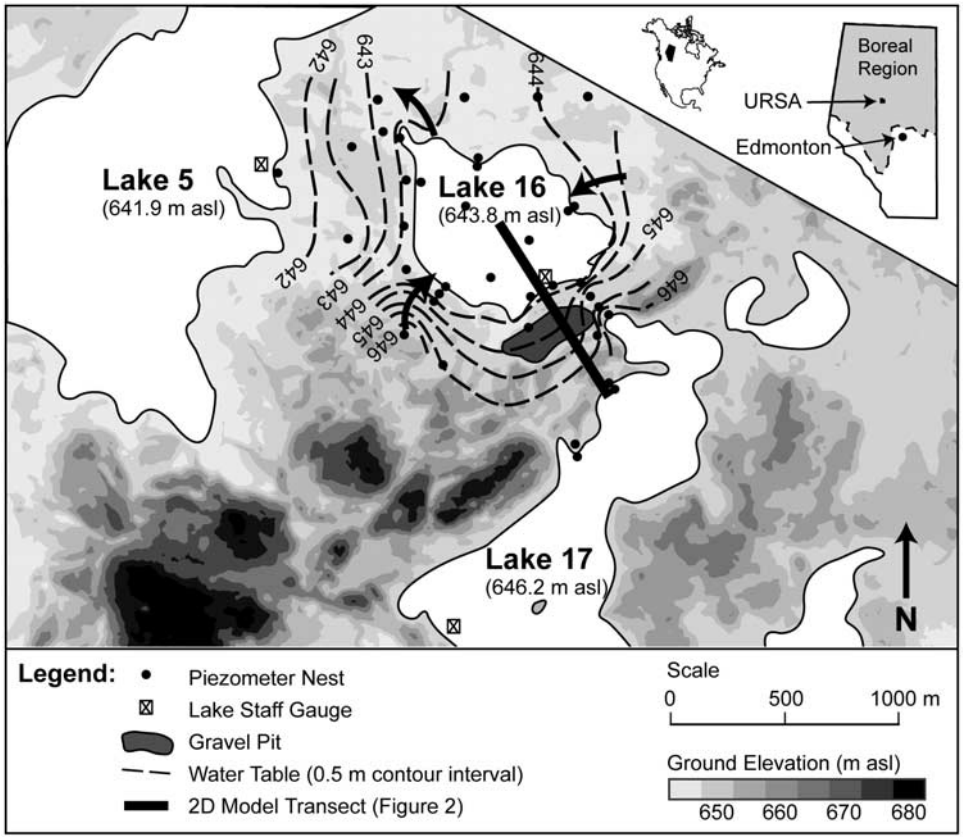

Figure 1. Lake 16 study site with ground surface topography, selected field instrumentation, and position of cross-sectional numerical model domain. Water table contours and groundwater flow direction groundwater flow direction shown for July 2002. Location of URSA and Boreal Plains region in Alberta, Canada shown on inset.

having different soil texture and vegetative land cover, and for upscaling site-specific knowledge to broader regions.

2. URSA Outwash Site

[5] The URSA is located in the Boreal Forest of Canada, 370 km north of Edmonton, Alberta, Canada (56°6′N, 116°32′W; Figure 1), and is characterized by a subhumid climate, thick heterogeneous glacial sediments [80 to 240 m; *Pawlowicz and Fenton*, 2002] overlying sedimentary bedrock, and subdued topographic relief. Within the URSA, landscape heterogeneity encompasses lacustrine plains, moraines, and an outwash plain. The outwash field site is situated on the eastern margin of a 200 km^2 coarse-textured glacial outwash plain. The plain is hummocky, has remnants of an east to west trending esker (indicated by elevated portions of Figure 1), and has a maximum topographic relief of 30 m. In the 1990s, a portion of the esker was excavated to supply mineral aggregate (sand and gravel) for local road development. As determined from periodic aerial photographs, available from the 1940s to 2002, most of the excavation occurred in 1996, and was limited to an oblong area between Lakes 16 and 17 (Figures 1 and 2).

[6] The outwash study site contains three lakes that exist in a series of ''steps'', where Lake 17 was 2.4 m higher than Lake 16, which was 1.8 m higher than Lake 5 in early 2002 (Figure 1). Measurements of hydraulic head at 70 piezometers, lake levels, and groundwater seepage estimates were made fro il 2001 to October 2003, as part of the water budget study presented by *Smerdon et al.* [2005]. Groundwater moved from southeast to northwest (Figure 1) at an average horizontal hydraulic head gradient of 0.002, with groundwater springs occurring along the southeast shore of Lake 16. In this study, the groundwater flow system between Lakes 17 and 16 is defined by hydraulic head data from a subset of 9 of the 70 piezometers between Lakes 17 and 16 (Figure 2). The stage of Lakes 16 and 17, and the water table elevation in the vicinity of the gravel pit (P8-W; Figure 2), were recorded with vented pressure transducers and dataloggers (Global-Water model WL-14) every 60 minutes. In this study, hydraulic head responses to rainfall events in summer 2002 were used as calibration data for transient simulations of groundwater recharge, and supported development of more generalized 1D recharge models.

[7] In north-central Alberta, annual precipitation varied from 318 to 529 mm from 1997 to 2001 [*Devito et al.*, 2005], and measured open water evaporation at the URSA varied from 336 to 438 mm from 1999 to 2003 [*Ferone and Devito*, 2004; *Smerdon et al.*, 2005], below the estimated annual average potential evapotranspiration (PET) of 518 mm reported by *Bothe and Abraham* [1993]. From 2001 to 2003, precipitation was recorded with a weight-recording gauge at a meteorological station 10 km west of the site, and was used in the 2D calibration models. Prior to 2001, the closest long-term meteorological station was in Slave Lake, Alberta (approximately 100 km

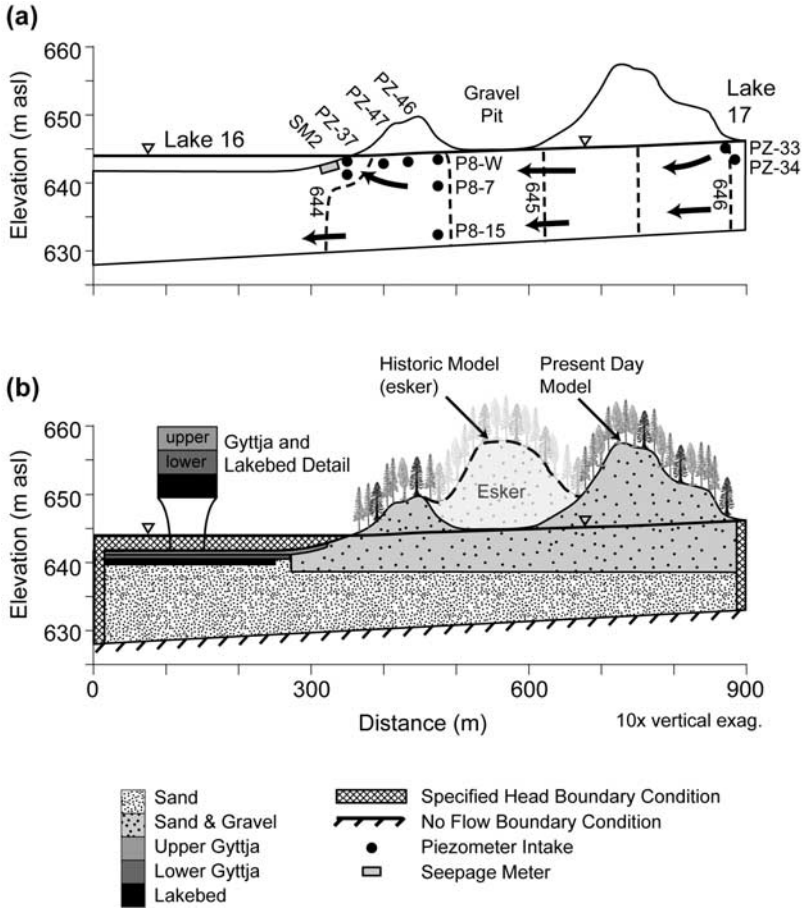

Figure 2. Cross section of the *Present Day* and *Historic* models (cross section location shown in Figure 1). (a) Field observation points and contours of simulated hydraulic head for July 2002. (b) Porous media zones (shaded), boundary conditions, and upland forested areas. Forested esker in Figure 2b is shaded lightly to illustrate the difference between each model.

south of the study site), and data were assumed to be indicative of regional climate conditions [*Environment Canada*, 2002] for long-term modeling. In this study, precipitation that occurred for the months of November through April was assumed to accumulate as snow, which is consistent with field observations and air temperature data.

3. Outwash Hydrologic Modeling

3.1. Conceptual Models

[8] Three-dimensional simulations of the outwash flow system [*Smerdon et al.*, 2007] identified values for the hydraulic parameterization of the outwash landscape, and illustrated that lake-groundwater interaction is controlled by highly permeable sandy sediments, riparian peatlands and stratified lakebed deposits. Successful simulation models of the hydrologic flow system required that climatic boundary conditions (i.e., precipitation and evaporation) be divided into forested and non-forested areas, and that the forested areas have three distinct timeframes (spring, summer and fall), corresponding to seasonal variation of throughfall and evapotranspiration [*Smerdon et al.*, 2007]. Water cycling was highly sensitive to the timing and magnitude of these seasonal periods of precipitation and evaporative fluxes. In t dy, simulation models were used to further investigate the sensitivity of groundwater recharge, driven by available long-term climate data in the region. Two-dimensional, cross-sectional models were used to examine the suitability of model parameters and determine lower-boundary conditions for development of 1D models. Thus the 2D models establish a link between prior 3D modeling efforts and more generic 1D recharge models, and consisted of:

[9] 1. *Present Day* model: a representation of the present day outwash landscape between Lakes 16 and 17, including the gravel pit, to validate parameterization of the 1D recharge models.

[10] 2. *Historic* model: a representation of the outwash landscape between Lakes 16 and 17 prior to excavation of the gravel pit, to investigate the influence of a forested canopy on the flow system and variability in water table position (i.e., to further justify boundary conditions for the 1D recharge models).

[11] Each conceptual model is presented in the following sections, with descriptions of the model configuration, boundary and initial conditions, and supporting field data. Simulations were completed with the HydroGeoSphere numerical code [*Therrien et al.*, 2005], which solves Richards' equation for transient, variably-saturated groundwater flow in a porous medium. The two-dimensional, cross-sectional model domains (location shown in Figure 1) were

(a)

Zone	K (m/s)	K_x:K_z	S_s (m^{-1})	ϕ
Sand	$1x10^{-5}$	10:1	10^{-5}	0.35
Sand & Gravel	$1x10^{-3}$	10:1	10^{-5}	0.35
Upper Gyttja	$3x10^{-6}$	1:1	10^{-4}	0.45
Lower Gyttja	$1x10^{-7}$	1:1	10^{-4}	0.45
Lakebed	$1x10^{-8}$	1:1	10^{-4}	0.45

(b)

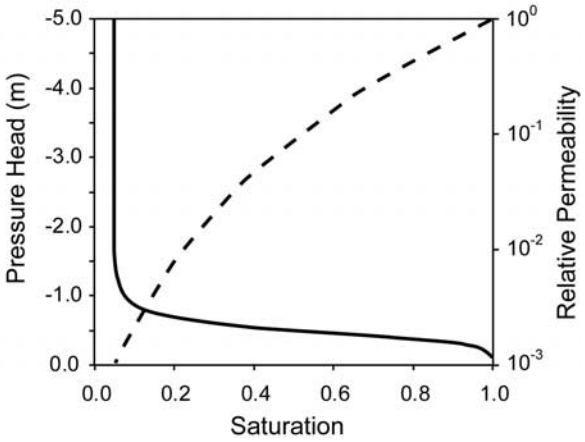

Figure 3. (a) Hydraulic parameters for each porous media zone and (b) pressure head and relative permeability curves for *sand and gravel zone*.

oriented parallel to groundwater flow, as determined by *Smerdon et al.* [2005]. Subsurface stratigraphy was represented by 5 different zones, based on interpretation of site geology [*Smerdon et al.*, 2005]. The hydrostratigraphy included division of the glacial outwash into an upper sand and gravel unit, and lower sand unit, which could not be represented in the spatial resolution of the 3D model by *Smerdon et al.* [2007]. Each zone was assigned hydraulic parameters, including a hydraulic conductivity (K) value, which was measured in the field, and estimates of specific storage (S_s), porosity (ϕ), and the ratio of horizontal to vertical hydraulic conductivity (i.e., K_x:K_z; Figure 3a). Tabulated relationships for capillary pressure, water saturation, and relative permeability were required, but were undetermined for these specific sandy outwash sediments. Consequently, on the basis of textural description and field observations by *Smerdon et al.* [2005], the parameters were assumed to be similar to those reported for the Borden sand [*Abdul*, 1985].

3.2. Canopy Interception and Actual Evapotranspiration

[12] A key finding from *Smerdon et al.* [2007] was that further investigation into the relationship between temporal throughfall and evapotranspiration fluid fluxes was necessary to define the rate and timing of groundwater recharge. Analysis of the recharge process depends on determining the relative partitioning of water to evapotranspiration, soil moisture storage, and deeper percolation. Such partitioning is governed by the complex, non-linear exchange of energy and moisture at the interface of the atmosphere and unsaturated zone. Actual evapotranspiration (AET) rates from aspen trees on sandy soil, and the transfer of moisture and energy across the forest canopy and forest floor (i.e., litter) have not been adequately characterized at the URSA.

[13] To compensate for this lack of data, actual evapotranspiration rates (Figure 4) were assumed to follow the seasonal rates determined by *Amiro et al.* [2006] for an aspen upland site in Prince Albert, Saskatchewan, Canada. The study by *Amiro et al.* [2006] was selected from a review of hydrologic and meteorological publications of evapotranspiration in boreal forests [*Redding et al.*, 2006] because of the similarity in climate, latitude (approximately 54°N, 106°W), forest canopy, and sandy soil texture as the Lake 16 study site. AET was represented as time-series fluid fluxes specified at the ground surface (i.e., sink for water; total of 400 mm yr^{-1}).

[14] Canopy interception was implemented as net precipitation: P_n (i.e., P_n = precipitation minus interception). P_n was assumed to be 90% of total precipitation, and represented forest canopy and litter interception. This value was based on a range of observed precipitation throughfall rates at the URSA (85% to 95% of P: K.J. Devito, unpublished data, 2005). For the historic regional climate record, where mean annual P was 455 mm yr^{-1}, mean annual P_n was 410 mm yr^{-1}.

[15] To assess the sensitivity of specified rates used in this study, AET and P_n were bracketed in each simulation with slightly higher and lower values. Daily AET values were increased or decreased such that the total annual AET was either 50 mm higher or lower than the *Base Case* (Figure 4). This range of AET (i.e., 350 to 450 mm yr^{-1}) spans variability observed by *Amiro et al.* [2006] in 2001 and 2002. P_n was bracketed by varying values to 85 and 95% of P. When combined the bracket rates (i.e., higher AET and lower P_n and a lower AET and higher P_n) represent the *Dry Case* and *Wet Case*, compared to the *Base Case* referred to in this study.

3.3. Present Day 2D Flow Model

[16] Simulation of the *Present Day* flow system was necessary to confirm the hydraulic parameters assigned to the zones of porous media [from *Smerdon et al.*, 2007], and the assumed AET and P_n values for the forested portions of the outwash landscape. Two separate time-

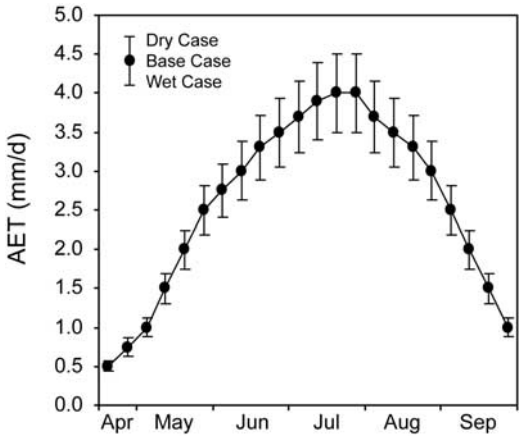

Figure 4. Specified weekly evapotranspiration (AET), based on the study of *Amiro et al.* [2006]. Solid dots represent values used in *Base Case* simulations, and the error bars denote *Dry* and *Wet Cases*.

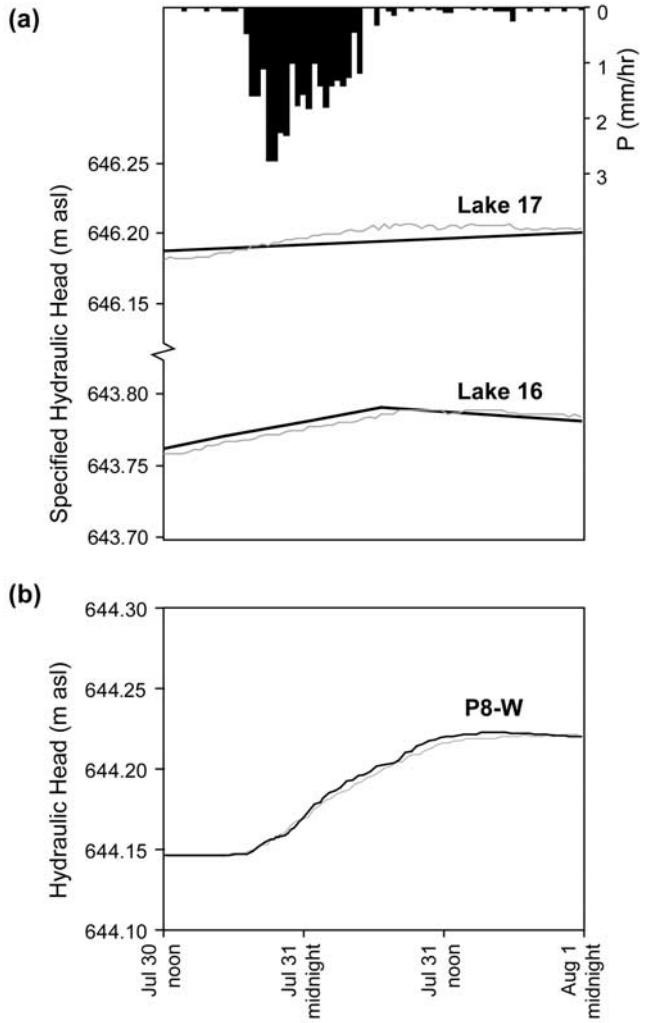

Figure 5. (a) Boundary conditions for *Present Day A* model, including precipitation and specified hydraulic heads for Lakes 16 and 17. Specified hydraulic heads for model input (thick black line) shown with the continuously recorded field data (thin gray lines). (b) Time-series of simulated (thick black line) and observed (thin gray line) hydraulic head response for P8-W.

frames were considered: July 30 to August 1, 2002, when a 35 mm rainfall event on July 31 resulted in an observed water table rise at P8-W (*Present Day A*); and, August 14 to September 18, 2002, when there were two rainfall events (25 mm and 45 mm) separated by approximately two weeks (*Present Day B*). For each scenario, the simulated transient water table response at P8-W was compared to time series of field data recorded with the pressure transducer and datalogger described earlier.

[17] The 2D model extended from the middle of Lake 16 to the edge of Lake 17 (Figures 1 and 2), in the principal direction of groundwater flow [*Smerdon et al.*, 2005, 2007]. The finite-element mesh was discretized spatially with elements spaced uniformly at 1 m in the horizontal direction, and variably spaced in the vertical direction (0.1 to 0.9 m), with finer vertical spacing occurring from the ground surface to a subs elevation below the position of the water table. The topography of the model domain was constructed from a 1 m horizontal resolution digital elevation model of the land surface combined with lake bathymetry measurements and interpretation of the bottom of the outwash sediments from geophysical data [*Domes*, 2004].

[18] Fluid flow boundary conditions included time-varying specified hydraulic heads of Lakes 16 and 17, which were defined at the left and right sides of the model domain, and lake area (Figures 2b, 5a, and 6a). The bottom of the mesh was set as a no-flow boundary because it corresponds with the base of the outwash deposits, which

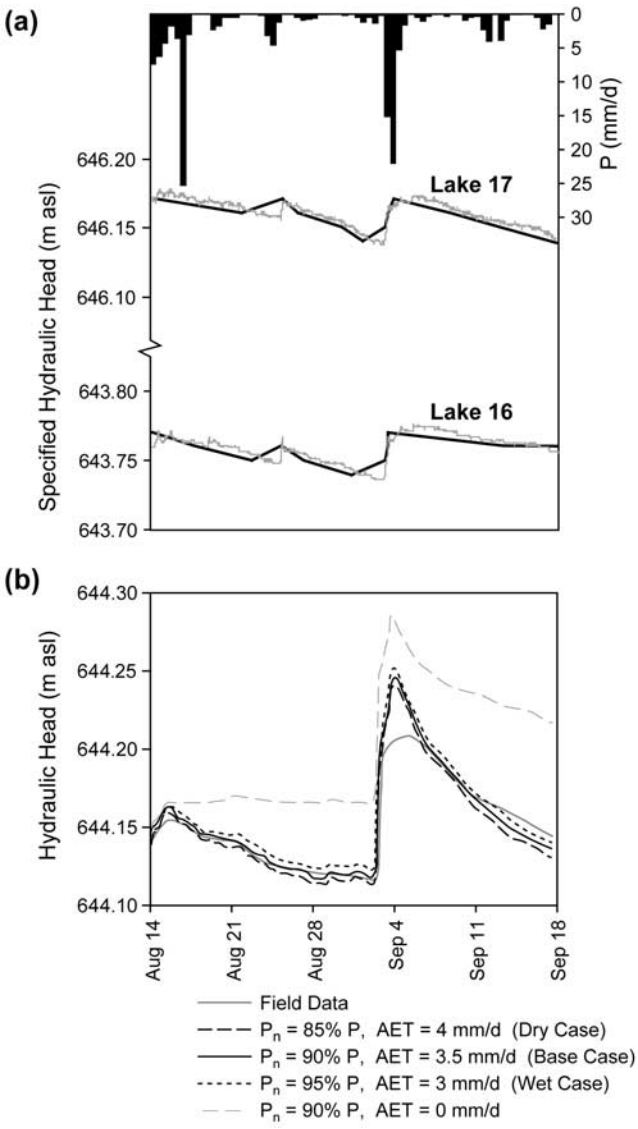

Figure 6. (a) Boundary conditions for *Present Day B* model, including daily precipitation and specified hydraulic heads for Lakes 16 and 17. Specified hydraulic heads for model input (thick black line) shown with the continuously recorded field data (thin gray lines). (b) Sensitivity of simulated hydraulic head response at P8-W to different P_n and AET values. The difference between field data and simulations for September 4 due to difference in precipitation recorded at rain gauge (10 km west of site) and location of P8-W.

are underlain by clay and have significantly lower hydraulic conductivity than the outwash sediments (Figure 3a). Initial hydraulic head and water saturation conditions were determined by running the model to equilibrium conditions with the specified head boundary conditions of Lakes 16 and 17 for July 30, 2002. These simulated initial conditions assumed that the average sum of atmospheric fluxes (i.e., P and AET) was zero, representing the long-term near equality of precipitation and evaporation for the region. Because of the high permeability of the sediments, this approach was successfully used to generate initial conditions in prior modeling at the URSA [*Smerdon et al.*, 2007]. Initial conditions were compared to field observations for each of the 9 selected observation points.

[19] Precipitation rates were applied as a time-series of fluid flux for each simulation (Figures 5a and 6a). Total precipitation (P) was applied to the ground surface of the gravel pit and net precipitation (P_n) was applied to the ground surface that was forested (Figure 2b). For the single 35 mm rainfall event (*Present Day A*), hourly precipitation data were specified and the simulated water table response was compared to observations to confirm subsurface hydraulic parameters (i.e., Figure 3). The rainfall event occurred in the evening, and to constrain evaluation of the water table response, AET and canopy interception were assumed to be negligible. For the *Present Day B* simulation, daily precipitation data and various combinations of assumed AET and interception rates were specified, as described in section 3.2. The simulated water table position at P8-W was compared to time-series field data obtained from the pressure transducer at this location, thereby using water table response to show that the assigned values are reasonable assumptions of AET and canopy interception.

3.4. Historic 2D Flow Model

[20] Using a similar model domain to that described above, hypothetical subsurface flow conditions were investigated for 1983 to 1996 by simulation. This period, which is prior to excavation of the gravel pit, was simulated to represent *Historic* water table behavior in response to net climatic fluxes (i.e., P_n minus assumed AET) recorded in the region for steady state and time-varying lake boundary conditions. The top surface of the model domain was assumed to include a forested esker, up to 10 m thick, which was subsequently removed (in 1996) to form the gravel pit (i.e., ground surface above 660 m asl in Figure 1; conceptualized section in Figure 2b). On the basis of aerial photographs and observations from the field, the esker topography was composed of linear, parallel ridges with linear, parallel depressions (i.e., not one continuous hill when viewed in cross section), caused by the formation of Lakes 16 and 17 from ice-block melting and slumping of adjacent esker sediments [*Pawlowicz and Fenton*, 2002]. The model used subsurface elements of the same spatial discretization as the *Present Day* model.

[21] To simulate the natural flow system prior to gravel pit excavation and to determine the sensitivity of the flow solution to lake boundary conditions, the flow system was simulated with: (1) average lake levels (i.e., steady state boundary conditions) and (2) monthly lake levels that fluctuated (i.e., transient boundary conditions). For each simulation, monthly climatic boundary conditions region for the region were input as net f uxes at the ground surface (i.e., P_n minus assumed AET), and the water table fluctuation was monitored at P8-W. Temporal AET rates were assumed to follow the distribution shown in Figure 4, and P_n was specified as 90% of P.

[22] Because this period of time occurred prior to field research at the URSA, lake levels were estimated from a simplified relationship between average monthly P, air temperature (data not shown), and potential evapotranspiration (PET) calculated by the method of *Thornthwaite* [1948] from historic data shown in Figure 7a. The net difference between P and PET was used to calculate an assumed change in lake level for each month (Figure 7b), assuming that lake level was entirely controlled by P and PET. That is, the monthly balance of other inputs and outputs, such as groundwater seepage were assumed to be zero.

[23] Observations at the Lake 16 study site [*Smerdon et al.*, 2005], and three-dimensional simulations of this lake-groundwater system [*Smerdon et al.*, 2007] have shown that the elevation of Lake 16 is dependent on groundwater discharge; however, the dominant hydrologic control is open water evaporation. Thus the objective of the *Historic* model was not to reconstruct the subsurface flow regime as accurately as possible, but rather to investigate the transient behavior caused by fluctuating lake levels when combined with assumed evapotranspiration rates. Considering the subhumid climate, we hypothesized that when the landscape was completely forested, groundwater recharge would be minimal and that the boundary Lakes 16 and 17 would largely control the water table position [*Haitjema and Mitchell-Bruker*, 2005]. These conditions would justify use of a static water table (lower) boundary condition in the following 1D models of groundwater recharge, which is often simulated as a unit-gradient boundary condition [e.g., *Scanlon et al.*, 2002].

3.5. 1D Recharge Models

[24] Long-term groundwater recharge, for water table depths varying from 2 to 12 m, was quantified by 1D models of unsaturated flow. These models allowed development of a more generic representation of groundwater recharge for coarse-textured deposits in this region than was possible with the 2D *Present Day* and *Historic* flow models. The series of *Recharge* models represent monolithic columns of unsaturated outwash sediment, extending upward from the water table to the ground surface.

[25] Each model had 0.2 m vertically spaced elements and varied in height from 2 to 12 m (incrementally increased by 1 m for a total of 11 separate columns), and were parameterized with the hydraulic properties of outwash sand and gravel (Figure 3). The upper boundary condition was defined by monthly P_n and the seasonal distribution of AET, respectively (Figure 8b). The lower-boundary condition was specified with a hydraulic head equal to the base elevation of the column to represent the (fixed) water table. Simulations were run with a variable time step of less than 1 month (depending on soil moisture conditions), and the fluid flux at the base of the column (i.e., the water table) was determined for 71 years (1933 to 2004). This approach was generally similar to that of *Keese et al.* [2005]; with the exception of different lower-boundary conditions, which were justified by the 2D simulations presented in this study. Initial conditions were set by allowing each model to run for 10 years prior to 1933 using precipitation data from the

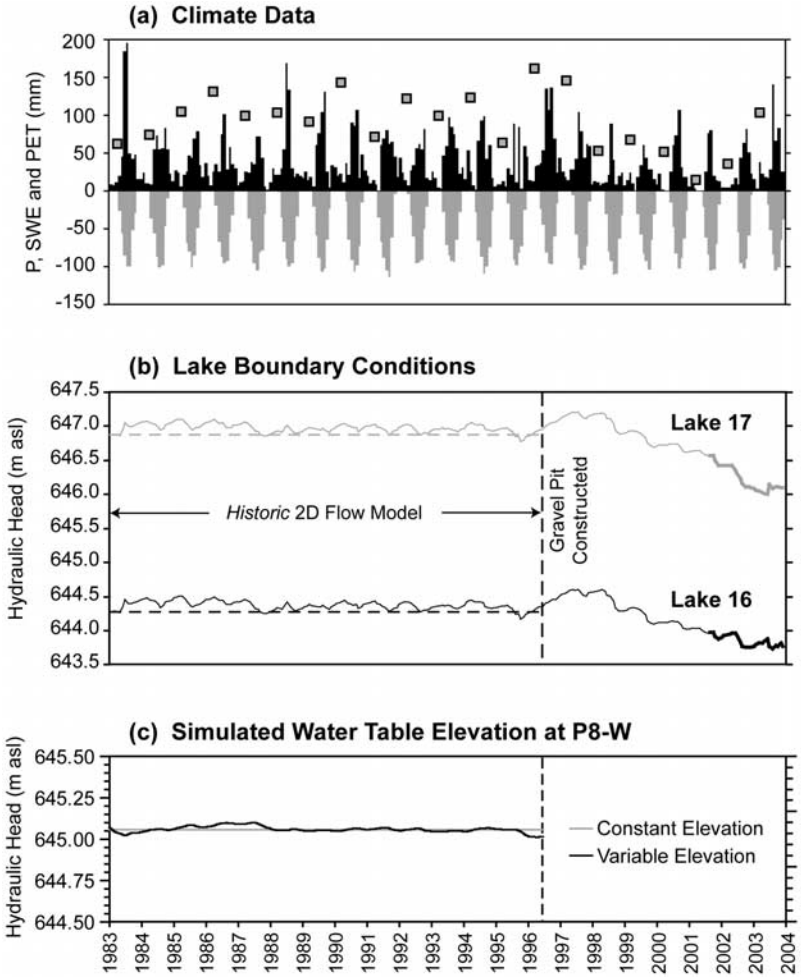

Figure 7. (a) Monthly precipitation, potential evapotranspiration (gray bars, calculated by the Thornthwaite method), and annual snow water equivalent, SWE (i.e., November to April precipitation expressed as mm, shown as squares). (b) Constant (dashed line) and time-varying (solid line) specified hydraulic head boundary conditions for *Historic* model. Variable lake elevations were estimated before 2001 (thin lines) and measured from 2001 to 2004 (thick lines). (c) Simulated water table elevation at P8-W for constant (gray line) and variable lake elevations (black line). The approximate time of gravel pit construction is denoted by vertical dashed line.

regional climate station (data not shown). The initialization timeframe (i.e., spin up) was chosen based on results from initial test simulations.

4. Results

4.1. Outwash Flow System (2D Models)

[26] Simulated initial conditions for the *Present Day* models were similar to field observations for July 2002 (Figure 9), having a root mean squared error (RMSE) of 0.16 m for hydraulic heads. Water table response of both the *Present Day A* and the *Present Day B* simulations compared well with field data (Figures 5b and 6b). The incorporation of a more permeable upper section of outwash sand and gravel improved the transient fit of simulated water table response to field observations at a finer temporal and spatial resolution than considered by *Smerdon et al.* [2007], and honored observations from subsurface investigations described by *Smerdon et al.* [2005]. Simulated water table response compared favorably with field observations when reasonable P_n and AET s were assumed (Figure 6b). The *Base Case* P_n and AET values provided a close match to field data and were bracketed by the *Wet* and *Dry Cases*. When AET was not considered, simulated hydraulic heads remained higher than observed in the field (Figure 6b: August 15 to 30, 2002), and replicated the transience of the imposed lake boundary conditions (Figure 6b: September 5 to 18, 2002).

[27] Results from the *Historic* model reveal that when the landscape was completely forested and composed of a thicker unsaturated zone, water table fluctuations at the present day monitoring point (P8-W) should have been less than 0.10 m, and controlled by the lake levels (Figure 7c). When Lakes 16 and 17 were simulated as constant level boundary conditions, the water table at P8-W remained at a constant level and did not respond to recharge originating at the ground surface (Figure 7c). However, following excavation of the gravel pit, the forest canopy (i.e., driver for AET) and unsaturated esker (i.e., depth to water table) were both reduced, and the water table responded to increased recharge (Figure 6b). Thus, for the 1D recharge models, implementation of a fixed

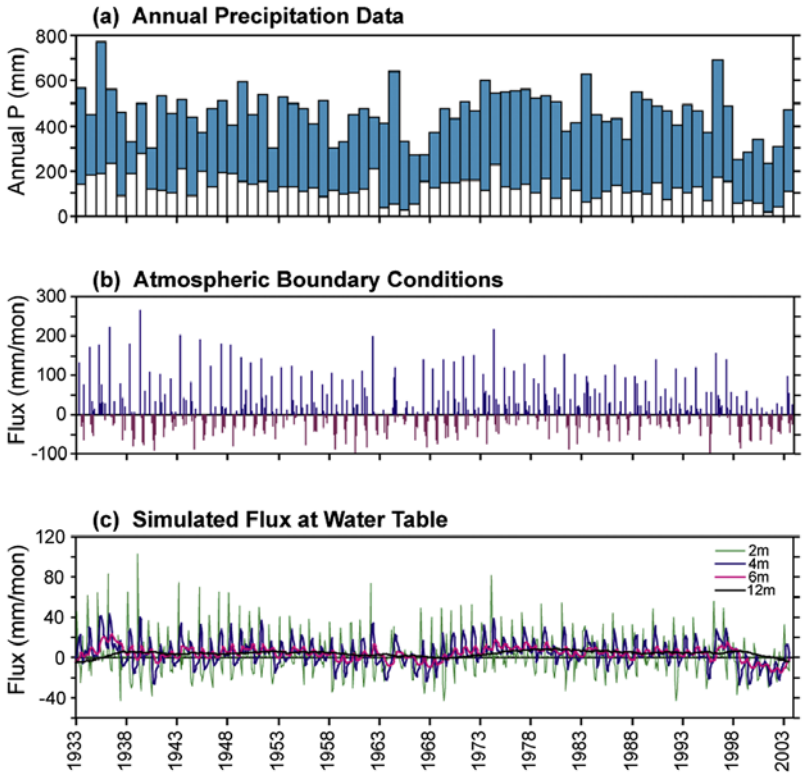

Figure 8. (a) Annual precipitation, separated into snow (white bars) and rainfall (blue bars). (b) Net monthly atmospheric boundary conditions for the *Base Case* (positive fluxes shown as blue bars, negative fluxes shown as pink bars). (c) Simulated monthly fluid fluxes for water table depths of 2, 4, 6, and 12 m below the ground surface.

water table as a lower-boundary condition was justified, and represents an alternative approach to the unit-gradient boundary condition that allows water to drain from the lower boundary [*Scanlon et al.*, 2002].

4.2. Groundwater Recharge (1D Hypothetical Models)

[28] Positive fluid fluxes at the water table indicate conditions when the saturated groundwater zone was a sink for infiltrating water (i.e., groundwater recharge), and negative values indicate conditions when the saturated groundwater zone was a water source [Herein referred to as upflux; *Jaber et al.*, 2006]. For the *Base Case*, a wide variation in monthly fluid flux was found for water table depths shallower than 6 m (Figure 8c). Generally recharge early in the year was followed by upflux later in the year, but the magnitude was dampened with increasing depth to the water table. This indicated that the amount of recharge and upflux largely depended on climatic boundary conditions of the present and immediately preceding year. For water table depths greater than 6 m, the seasonality of positive and negative fluxes and influence of climatic conditions became increasingly dampened (e.g., consider 12 m: Figure 8c), and monthly groundwater recharge rates decreased to less than 10 mm. Upflux conditions occurred only infrequently.

[29] The relationship between climatic conditions and flux at the water table is clearly illustrated for the late 1960s period, when moisture deficit conditions from 1963 to 1966 (Figure 8c) were followed by moisture surplus conditions from 1967 to 1972 (Figures 8c and 10a). Prior to the onset of moisture surplu itions in 1967, simulated groundwater recharge was negligible (<10 mm month^{-1}), with 10 to 25 mm month^{-1} of upflux occurring in the summer months. At the onset of moisture surplus conditions (Figure 10a), simulated groundwater recharge occurred within the same year for water table depths of 2 and 4 m, but there was a delayed increase in recharge at greater

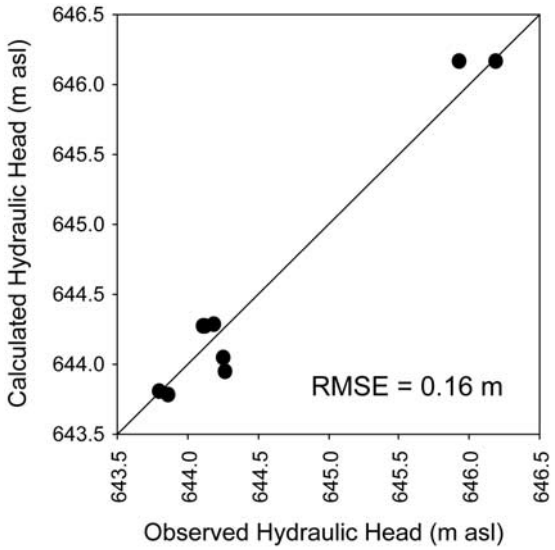

Figure 9. Simulated hydraulic heads for July 2002 compared to field data. Root mean squared error (RMSE) shown for 9 observations points.

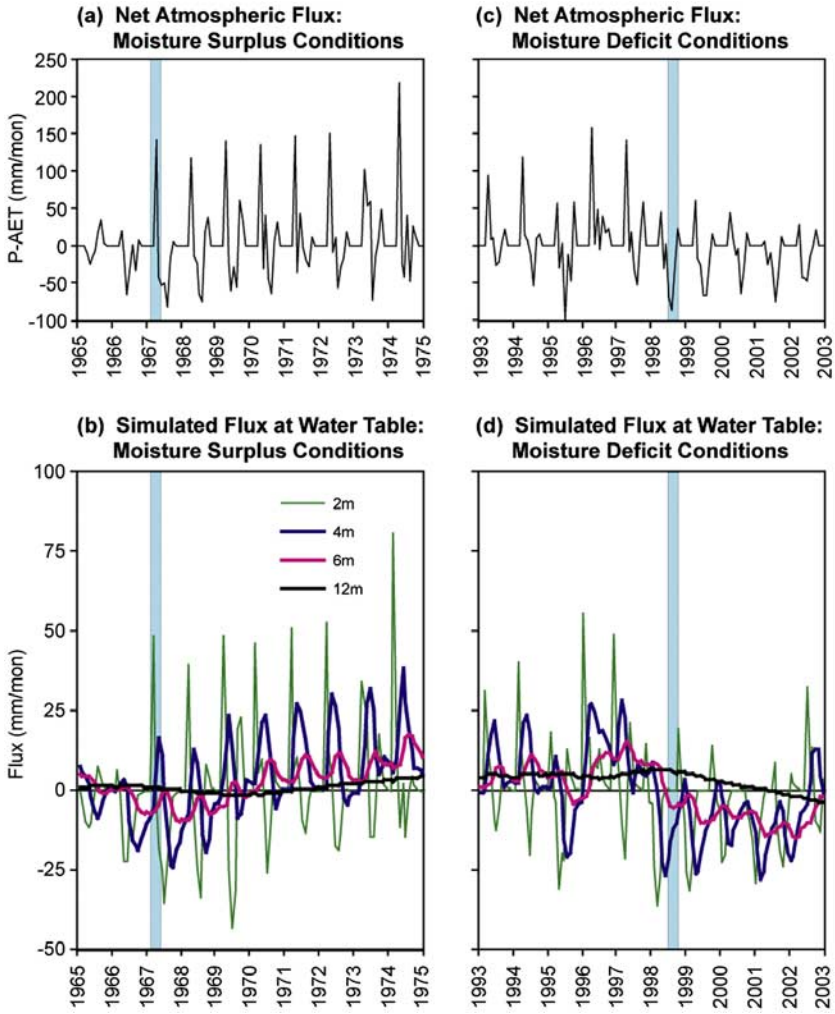

Figure 10. Net atmospheric flux and simulated flux at water table depths of 2, 4, 6, and 12 m shown in Figures 10a and 10b for the onset of moisture surplus conditions in 1967 (identified by blue shaded bar). Net climatic flux and simulated water table fluxes shown in Figures 10c and 10d for moisture deficit conditions beginning in 1998 (identified by blue shaded bar).

depths. Analysis of annual precipitation (Figure 8a) reveals that normal snow thickness was approximately 100 mm yr^{-1} and between 1963 and 1966 annual snow accumulation was less than 50 mm yr^{-1}, which was less than average for the 71 year timeframe. Moisture surplus conditions were created by a return to normal thickness of snow accumulation and an increase in precipitation in the spring months of 1973 (251 mm) and July 1974 (150 mm). However, the simulated increase in groundwater recharge, associated with moisture surplus conditions, was delayed by 2 and 3.5 years for water table depths of 6 and 12 m (Figure 10b), respectively, indicating a strong time-lagged response.

[30] Although unsaturated mass transport processes were not explicitly simulated in this study, and soil moisture content would vary during simulated timeframe, the simple procedure of tracking a hypothetical tracer (assuming residual moisture content) established approximate travel times. The conservative tracer was considered as a means to further illustrate and quantify the time-lagged response. Considering the onset of moisture surplus conditions illustrated in Figures 10a and 10b, a rate of movement of a tracer front originatin at the ground surface may be determined by dividing the cumulative, net monthly flux (Figure 8b) by the residual moisture content of the porous media (approximately 0.05; Figure 3). The resulting time-series graph (Figure 11) illustrates the vertical movement of a tracer in the unsaturated zone, and confirms the predicted time-lagged response of flux at the water table. For the same development of moisture surplus conditions, movement from the ground surface to a shallow water table (2 m) requires about 1 year (Figure 11a). For water table depths of 6 and 12 m, approximately 4 and 7 years were required.

[31] The time-lag response was also observed when moisture surplus conditions shifted to deficit conditions in 1998 (Figure 10c). A decline in annual snow accumulation (to approximately 65 mm yr^{-1} from 1998 to 2000) caused recharge to diminish in 1998 for water table depths of 2 and 4 m (Figure 10d). However, the moisture deficit (drought) conditions were found to decrease recharge for water table depths of 6 and 12 m within 1.5 and 2 years, respectively. Compared to development of moisture surplus conditions (in the late 1960s), the onset of drought appeared to have a time-lag that was shorter by approximately 1 year.

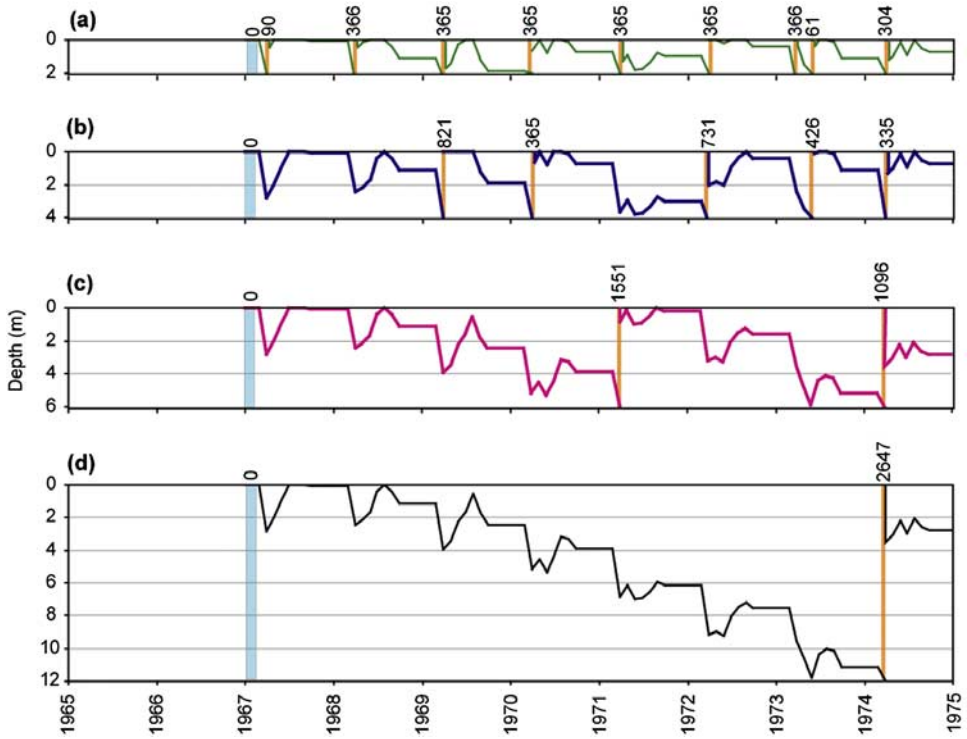

Figure 11. Simulated movement of a tracer initiated at the ground surface in 1967 (blue shaded bar). Position of the tracer in the unsaturated zone is shown throughout development of the moisture surplus conditions illustrated in Figure 10a, for water table depths of 2, 4, 6, and 12 m in Figures 11a to 11d. Orange vertical lines identify the migration time from ground surface to the water table.

[32] Differences in time-lag between moisture surplus and moisture deficit could be caused by the magnitude of surplus/deficit or by differences in the wetting and drying process and soil moisture distribution. In each precipitation forcing scenario (i.e., moisture surplus and deficit), annual snow accumulation changed by approximately 40 to 50 mm. Considering that the sandy outwash is generally well drained, and the shift to drought conditions occurred with a shorter time-lag than a corresponding shift to wet conditions, the differences in time-lag illustrate the effect that annual evaporation has on wetting and drying. Propagation of slightly higher-moisture conditions to water table depths of 6 m of more (i.e., development of recharge), was controlled by gravity drainage and annual evaporation. Because there was a slight surplus in moisture, and the soil was wetting, flux at the water table eventually increased (Figure 10b). However, the equivalent forcing scenario for drying conditions was dominated by the annual evaporation and occurred with time-lag. The effect of drought in the late 1990s and early 2000s resulted in upflux conditions being favored over groundwater recharge, with 25 mm month^{-1} of upflux simulated for a water table depth of 4 m in nearly every year from 1998 to 2003 (Figure 10d).

4.3. Net Effect on Annual Fluid Fluxes

[33] The net effect on water cycling in coarse-textured landscapes, and the sensitivity to slightly wetter and drier conditions (represented by the *Wet* and *Dry Cases*), was apparent at annual (or longer) timescales (Figure 12). Although there are frequent years of moisture deficit conditions, annual net fluxes at the ground surface favor moisture surplus conditio ure 12a), as expected in a subhumid climate. At shallow water table depths (i.e., 2 m), the large monthly variability of fluid fluxes (Figure 8c) was reduced at the annual timescale (Figure 12b). The net effect was less variation in annual recharge for a 2 m deep water table (up to 149 mm), compared to the 4 m depth (up to 266 mm), indicating a higher sensitivity to atmospheric moisture conditions for areas with a shallow water table. These findings illustrate the role of climate on soil moisture in the upper 4 m of the unsaturated zone (Figures 8 and 12). For a water table depth of 12 m, groundwater recharge conditions occurred through much of the simulation period, annual variability was dampened, and there appeared to be a 30 to 40 year period between minimum and maximum rates (Figure 12e). For the *Base Case*, the net recharge was between 60 to 100 mm yr^{-1} from 1938 to 1958, and from 1978 to 1998.

[34] Summary statistics (mean, standard deviation, and skewness) for annual data indicated that mean recharge increased from 16 to 50 mm yr^{-1} for water table depths of 2 to 4 m, and was 45 mm yr^{-1} for water depths of 6 m or more (Figure 13a). These data illustrate 3 distinct groups that correspond to increasing water table depth: up to 4 m, with a normal distribution and mean of 16 mm yr^{-1}; 4 to 5 m, with average annual recharge up to 50 mm yr^{-1} and relatively high standard deviation (63 to 85 mm); and, 6 m or more, which is characterized by mean recharge of 45 mm yr^{-1}, and decreasing standard deviation and skewness with increasing depth to water table. Analysis of 10 mm interval histograms for each depth revealed that although the mean was 45 mm yr^{-1}, peak recharge values were 60 mm yr^{-1} for water table depths 9 m or greater. These

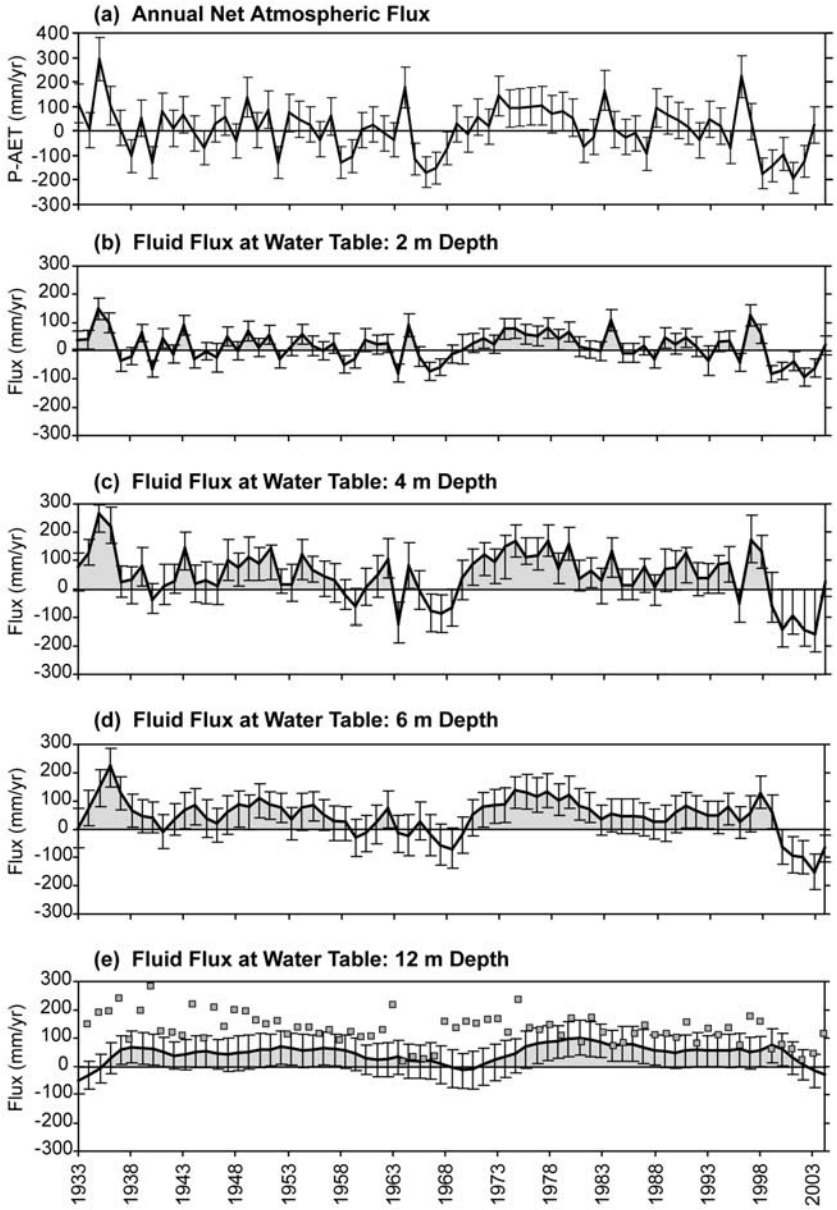

Figure 12. (a) Net annual atmospheric boundary conditions (i.e., precipitation minus actual evapotranspiration) for 1D models. (b) to (e) Simulated fluid fluxes at the water table for unsaturated thicknesses of 2, 4, 6, and 12 m, with duration of groundwater recharge shaded (gray). Solid lines represent the *Base Case* and error bar limits denote results of *Dry* and *Wet Cases*. Annual snow water equivalent from Figure 8a shown as squares in Figure 12e.

annual data can also be summarized as cumulative probability distributions (Figure 14), which indicate that the probability for recharge conditions increases to approximately 0.8 with increasing depth to water table.

5. Discussion

5.1. Effect of Subhumid Climate and Forest Cover on Recharge

[35] In subhumid regions, climate can vary from water deficit to water surplus conditions at monthly and decadal timescales and is a dominant factor in determining the magnitude of water available for groundwater recharge. When forested land cov onsidered, seasonal variation of P_n and AET controls the occurrence of recharge or upflux conditions, and ultimately constrains the flux of water at the water table. On coarse-textured landforms, the maximum potential for groundwater recharge will occur when the influence of AET was limited, such as during spring melt (when the forest canopy has not developed much leaf area coverage), and in the fall months. *Gosselin et al.* [1999] had similar findings for a site in Nebraska, where groundwater recharge was greatest between growing seasons. Within the growing season, groundwater recharge may be possible; however, the occurrence of recharge is limited to periods in the summer months when extreme precipitation events significantly exceed canopy interception and AET (e.g., 1996 in Figures 8a, 12c, and 12d).

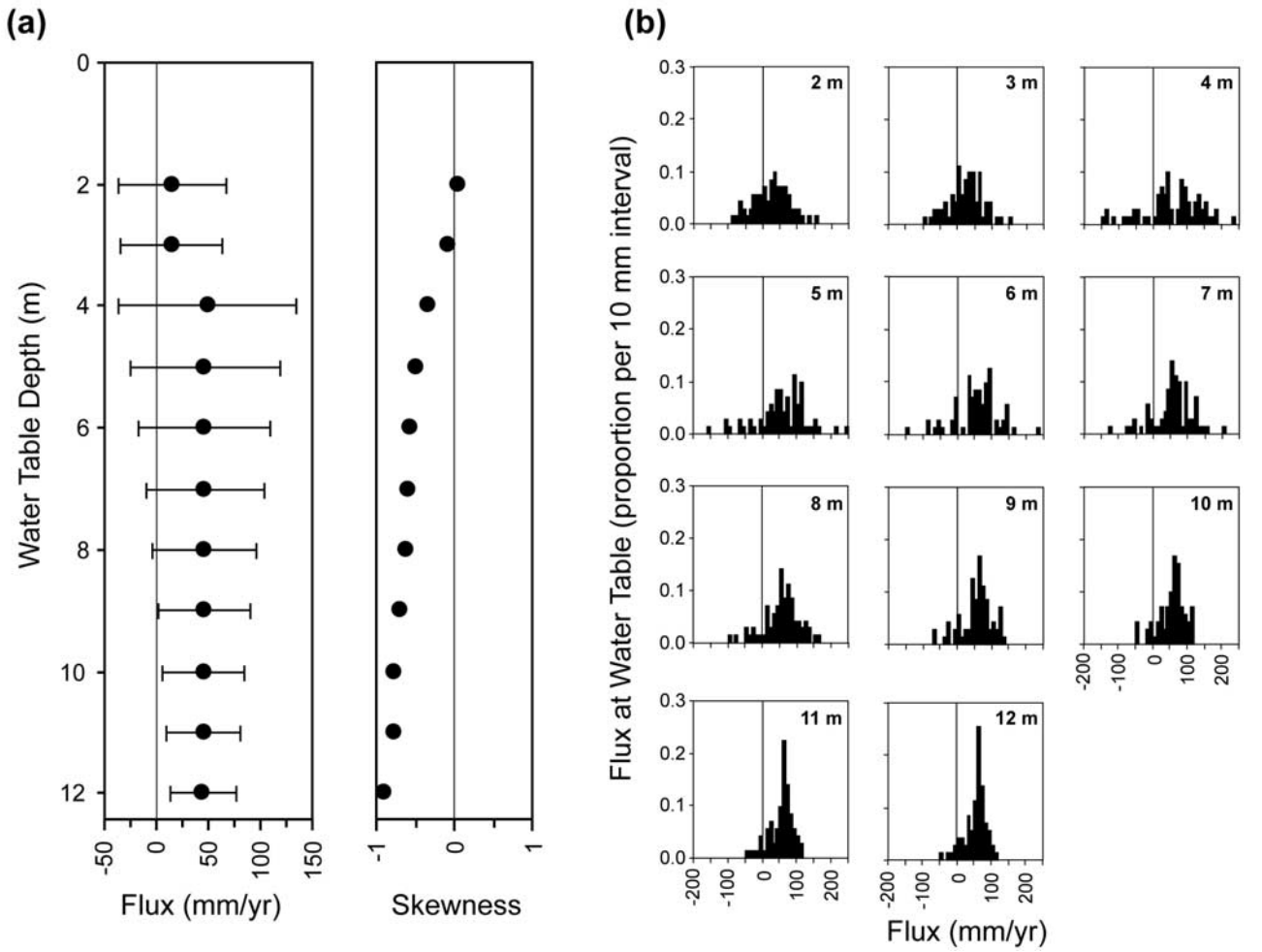

Figure 13. (a) Summary statistics (mean, standard deviation, and skewness) and (b) 10-mm interval histograms of annual water table flux data for each 1D recharge model.

[36] For hypothetical models of recharge to glacial outwash aquifers presented in this study, two intervals of water deficit conditions (drought) occurred in the late 1960s and in the late 1990s (Figure 12a), and appeared to be caused by decreased snow accumulation (Figure 8a). Each of these drought conditions resulted in diminished groundwater recharge and increased upflux from the water table (Figure 10), a hydrological process which has been measured at up to 40 mm yr^{-1} in humid regions with agricultural land use [*Jaber et al.*, 2006]. The reliance of groundwater recharge on snowmelt and/or large summer precipitation events is illustrated further in the moisture surplus conditions of the early 1970s (Figure 10b), and relatively high precipitation of 1996 (Figure 10d), and when a water table depth of 12 m was considered. In each of these scenarios there appeared to be a strong relationship between annual snow accumulation and long-term groundwater recharge (Figure 12e).

[37] Thus, for coarse-textured, forested landscapes in subhumid regions, the occurrence of recharge will depend on year-to-year variations in weather, especially annual snow accumulation. After the snowmelt recharge event, the forested portions of the landscape can remove water though AET and a decrease in recharge is followed by

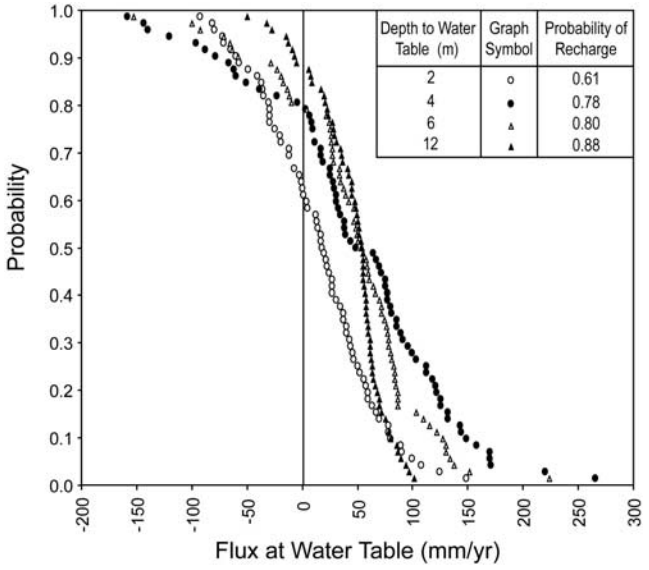

Figure 14. Probability of exceeding minimum fluid flux for water table depths of 2, 4, 6, and 12 m. Positive values indicate conditions of groundwater recharge and negative values indicate conditions of upflux from the water table.

upflux conditions in the summer months. Large summer precipitation events may have the potential to generate recharge to the groundwater regime; however, snow accumulation and subsequent rapid melting in the spring occur prior to the moisture demands and interception of a forested landscape.

5.2. Variation in Recharge With Water Table Depth

[38] Hummocky topography and coarse-textured glacial outwash often result in a water table that is nearly horizontal between lakes [*Winter*, 1986], which adds complexity to the prediction of spatial distributions of groundwater recharge. As illustrated along the cross section (Figure 2), the depth to water table for the URSA outwash site may vary from 0 to 12 m. Areas of shallow water table depth (i.e., 2 to 3 m) have a potential for recharge and upflux conditions monthly, and the magnitude will depend on the amount of snowmelt and large precipitation events in the current year. In a semi-arid region having annual P of 340 mm (similar to deficit years at the URSA), *Cook et al.* [1989] found that most rainfall was captured by AET in the uppermost 2 m of the soil column. For a 2 m deep water table, the long-term simulations of the present study indicate that upflux rates were as high as 92 mm month^{-1} in drought years. As the depth to water table increased, the annual variability of groundwater recharge decreased (Figures 12 and 13), illustrating that a thicker unsaturated zone provides is greater opportunity for infiltration below an extinction depth for evaporation [*Shah et al.*, 2007].

[39] The magnitude of groundwater recharge at monthly or annual timescales was shown to depend on the thickness of the unsaturated zone (i.e., the depth to the water table; Figures 8c and 12). Thicker unsaturated zones are associated with lag-times (Figure 11) that have the potential to record many years of changes in moisture and salt profiles [*Scanlon et al.*, 2007]. Thus the influence of differences in annual climate will have varying results on groundwater recharge, depending on the thickness of the unsaturated zone. The probability of groundwater recharge was estimated to be about 0.6 for shallow water table depths, and about 0.8 to 0.9 for water table depths of 6 m or more (Figure 14). This study illustrated that the onset of moisture surplus conditions would require approximately 4 years to reach a 6 m deep water table and 7 years to reach a 12 m deep water table (Figure 11). The differences in lag-time can be attributed the characteristics of the soil texture, which govern the infiltration processes following drought.

[40] However, when average conditions are considered, 3 distinct depths ranges emerge for recharge/upflux conditions (Figure 13). In areas of shallow water table depth (2 to 3 m), the probability of recharge or upflux is nearly equal, having a mean recharge of only 16 mm yr^{-1}. The largest standard deviation in recharge/upflux (85 mm) was predicted for water table depths of 4 to 5 m, suggesting that a threshold for recharge occurs at approximately 4 m (Figure 13a). This threshold depth is similar to the modeled evaporative extinction depths predicted by *Shah et al.* [2007] for forest cover on sandy soils (3.3 m), and illustrates the transition between potential for upward moisture migration by capillary forces at shallower depths, and percolation by gravity drainage with increasing depth to water table. Threshold-type behavior has been observed by *Redding and Devit* 08] for shallow soils at a moraine site at the URSA, and may form as part of the balance between transient soil moisture conditions of the uppermost portion of the soil columns [as suggested by *Cook et al.*, 1989] and deeper percolation. Further field investigation and modeling of root zone hydraulics is required to determine where thresholds occur on different landforms.

[41] Water balance models such as HELP [*Schroeder et al.*, 1994] have aided the quantification of distributed groundwater recharge by integrating spatially variable land cover and common climatic variables [e.g., *Jyrkama et al.*, 2002; *Scibek and Allen*, 2006]. However, specification of a static evaporative depth in HELP eliminates prediction of the transient upflux/recharge conditions (i.e., a dynamic evaporative depth, dependent on climate and soil moisture history) as identified by *Scanlon et al.* [2002], and confirmed in the present study. Groundwater recharge rates were not found to be steady, and variation appeared to follow average climate conditions from the most recent decade, and whether there were extended periods of water deficit or surplus, compared to periods of near balance. These transient results corroborate the findings of only a weak relationship between mean annual temperature (indicative of recent climate conditions) and recharge by *McMahon et al.* [2006], and suggest that recharge and/or upflux could be simulated in one-dimension using atmospheric flux data and knowledge of soil profiles for a region based on approximate/average water table depth.

5.3. Variation in Soil Texture and Vegetation Type

[42] Rates of recharge and upflux (Figures 10 and 12), the associated summary statistics (Figure 13), and cumulative probability distribution (Figure 14) were developed from an extension of field observations of water table response to specific precipitation events to generalized 1D models. These models link forest canopy interception, evapotranspiration, and groundwater recharge for one soil texture, which has a relatively high K (1×10^{-3} m s^{-1}), and a given relationship for capillary pressure, water saturation, and relative permeability. Variation in the parameterization of this soil texture will result in different unsaturated flow characteristics, which could yield different predictions of groundwater recharge. Considering the relatively high K of the outwash sand and gravel deposit, we anticipate that sediments with higher K will exhibit infiltration characteristics similar to those predicted in this study (i.e., seasonal recharge driven by snowmelt, and development of upflux conditions in shallow water table areas following drought). A sensitivity analysis, including more realistic representation of root zone and AET processes, would be needed to further investigate these variations.

[43] Although actual evapotranspiration was not explicitly modeled for the climate data in this study, reasonable AET values for a similar Boreal Forest site were specified. The relationships between atmospheric conditions, soil moisture and vegetation are complex, and actual evapotranspiration rates will vary annually depending on climate and soil moisture conditions, and the growth stage of the vegetative cover. For the 71 year timeframe considered in the one-dimensional infiltration models, AET rates would have varied depending on age of the forested ecosystem, density of trees and other vegetation, and climate conditions. As additional knowledge of site specific AET processes is acquired, future models of the coupled relationship between

energy and moisture transfer could be developed, and could explicitly consider succession of vegetative species for simulation of multiple decades and climate cycles.

6. Conclusions

[44] Rates of groundwater recharge are largely driven by snowmelt, and have been shown to depend on year-to-year variation in climate and the depth to the water table. The present year, the preceding year, or the past decade will control the amount of recharge or upflux. This study echoes conclusions of similar modeling analyses in different climate regions and considering different soil texture, which illustrate that understanding the groundwater recharge process depends on understanding the synchronicity of precipitation events compared to seasonal AET. The subhumid climate, with inter-annual and longer-term variation between water surplus and water deficit conditions, causes both groundwater recharge and upflux from the water table to occur within a single year for areas with a shallow water table. Recharge rates will depend on the current and previous year for water table depths of 4 to 5 m or less. At depths greater than 5 m, recharge will depend on climate conditions from the most recent decade.

[45] Fluid fluxes at the water table (recharge or upflux) were sensitive to small changes in annual climatic boundary conditions, especially in areas where the water table was shallow. The relationship between recharge (and upflux) to water table depth has implications for larger-scale hydrologic modeling on the Boreal Plains, and the cumulative probability distribution presented for distinct depth ranges will aid capturing site-specific knowledge and spatiotemporal variability in larger-scale regional models. Detailed knowledge of ground surface topography may be useful for defining areas where the water table is expected to be shallow (i.e., <5 m depth), which will have more dynamic recharge/upflux functions than areas with deep water tables. However, considering that surface water features, such as wetlands, ponds and lakes, control the configuration of the water table, lower-resolution DEMs could be used, thus increasing the availability of resources for field-level reconnaissance.

[46] The recharge rates predicted in this study, and summary statistics, add to a growing understanding of water cycling in subhumid regions of the Boreal Forest. The methodology described in this study is similar to other approaches for modeling groundwater recharge; however we have illustrated conditions where upward movement of soil moisture may develop from multi-year drought, which requires definition of a water table boundary. Recharge and/or upflux could be simulated for areas of common soil properties and water table depth using atmospheric flux data and knowledge of soil profiles for a large region. Combined with summary statistics or probability distributions, subsequent application in watershed models could be used to investigate changes in water cycling following land use changes (e.g., reclamation of open pit mines and harvested forest areas), influence of climate change, and to assess the effect of forest fire.

[47] **Acknowledgments.** Funding for this research project was provided through an NSERC-IPS to B. D. Smerdon (sponsored by Syncrude Canada Ltd.), NSERC Discovery grants to K. J. Devito and C. A. Mendoza, an NSERC-CRD grant for the HEAD Project, and an NSERC-CRD grant with Syncrude Canada Ltd., Circumpolar/Boreal Alberta Research (C/BAR) grants to B. D. Smerdon, and Institute for Wetland and Waterfowl Research (IWWR) grants to B. D. Smerdon and K. J. Devito. We acknowledge R. Therrien and E. A. Sudicky for use of the HydroGeoSphere code, R. McLaren for the GridBuilder mesh generator, and I. Creed for access to high-resolution DEM data for the URSA. Comments from A. Porporato, A. Guswa, and four anonymous reviewers greatly improved earlier versions of this manuscript.

References

Abdul, A. S. (1985), Experimental and numerical studies of the effect of the capillary fringe on streamflow generation, Ph.D. thesis, 210 pp., University of Waterloo, Waterloo, ON.

Amiro, B. D., et al. (2006), Carbon, energy and water fluxes at mature and disturbed forest sites, Saskatchewan, Canada, *Agric. For. Meteorol.*, *136*, 237–251.

Anderson, M. P., and J. A. Munter (1981), Seasonal reversals of groundwater flow around lakes and the relevance to stagnation points and lake budgets, *Water Resour. Res.*, *17*, 1139–1150.

Bothe, R. A., and C. Abraham (1993), Evaporation and evapotranspiration in Alberta, 1986–1992 Addendum, Alberta Environmental Protection, Edmonton, AB.

Cook, P. G., G. R. Walker, and I. D. Jolly (1989), Spatial variability of groundwater recharge in a semiarid region, *J. Hydrol.*, *111*, 195–212.

de Vries, J. J., and I. Simmers (2002), Groundwater recharge: An overview of processes and challenges, *Hydrogeol. J.*, *10*, 5–17.

Devito, K. J., I. F. Creed, and C. J. D. Fraser (2005), Controls on runoff from a partially harvested aspen-forested headwater catchment, Boreal Plain, Canada, *Hydrol. Processes*, *19*, 3–25.

Domes, F. (2004), 2-D traveltime inversion of near surface refractions and reflections in support of hydrogeological studies, Diploma. Karlsruhe University, Germany.

Environment Canada (2002), 2002 Climate Data CD West. (Available at http://climate.weatheroffice.ec.gc.ca/prods_servs/cdcd_iso_e.html)

Ferone, J. M., and K. J. Devito (2004), Shallow groundwater-surface water interactions in pond-peatland complexes along a Boreal Plains topographic gradient, *J. Hydrol.*, *292*, 75–95.

Gosselin, D. C., S. Drda, F. E. Harvey, and J. Goeke (1999), Hydrologic setting of two interdunal valleys in the Central Sand Hills of Nebraska, *Ground Water*, *37*, 924–933.

Haitjema, H. M., and S. Mitchell-Bruker (2005), Are water tables a subdued replica of the topography?, *Ground Water*, *43*, 781–786.

Jaber, F. H., S. Shukla, and S. Srivastava (2006), Recharge, upflux and water table response for shallow water table conditions in southwest Florida, *Hydrol. Processes*, *20*, 1895–1907.

Jyrkama, M. I., J. F. Sykes, and S. D. Normani (2002), Recharge estimation for transient ground water modeling, *Ground Water*, *40*, 638–648.

Keese, K. E., B. R. Scanlon, and R. C. Reedy (2005), Assessing controls on diffuse groundwater recharge using unsaturated flow modeling, *Water Resour. Res.*, *41*, W06010, doi:10.1029/2004WR003841.

McMahon, P. B., K. F. Dennehy, B. W. Bruce, J. K. Bohlke, R. L. Michel, J. J. Gurdak, and D. B. Hurlbut (2006), Storage and transit time of chemicals in thick unsaturated zones under rangeland and irrigated cropland, High Plains, United States, *Water Resour. Res.*, *42*, W03413, doi:10.1029/2005WR004417.

Pawlowicz, J. G., and M. M. Fenton (2002), Drift thickness of the Peerless Lake map area (NTS 84B), *Map 253*, Alberta Geological Survey, Edmonton, Alberta, Canada.

Redding, T. E., and K. J. Devito (2008), Lateral flow thresholds for aspen forested hillslopes on the Western Boreal Plain, Alberta, Canada, *Hydrol. Processes*, doi:10.1002/hyp.7038, in press.

Redding, T. E., B. D. Smerdon, S. Kaufman, and J. R. vanHarlem (2006), Evapotranspiration from Boreal forests: A summary of methods and flux rates, Literature review. Western Boreal Forest Hydrology Research Group, University of Alberta, Edmonton, AB.

Scanlon, B. R., M. Christman, R. C. Reedy, I. Porro, J. Simunek, and G. N. Flerchinger (2002), Intercode comparison for simulating water balance of surficial sediments in semiarid regions, *Water Resour. Res.*, *38*(12), 1323, doi:10.1029/2001WR001233.

Scanlon, B. R., R. C. Reedy, and J. A. Tachovsky (2007), Semiarid unsaturated zone chloride profiles: Archives of past land use change impacts on water resources in the southern High Plains, United States, *Water Resour. Res.*, *43*, W06423, doi:10.1029/2006WR005769.

Schroeder, P. R., T. S. Dozier, P. A. Zappi, B. M. McEnroe, J. W. Sjostrom, and R. L. Peyton (1994), The hydrologic evaluation of landfill performance (HELP) model: Engineering documentation for version 3, EPA/

600/R-94/168b, U.S. Environmental Protection Agency Office of Research and Development, Washington, D.C.

Scibek, J., and D. M. Allen (2006), Modeled impacts of predicted climate change on recharge and groundwater levels, *Water Resour. Res.*, *42*, W11405, doi:10.1029/2005WR004742.

Shah, N., M. Nachabe, and M. Ross (2007), Extinction depth and evapotranspiration from ground water under selected land covers, *Ground Water*, *45*(3), 329–338.

Smerdon, B. D., K. J. Devito, and C. A. Mendoza (2005), Interaction of groundwater and shallow lakes on outwash sediments in the sub-humid Boreal Plains of Canada, *J. Hydrol.*, *314*, 246–262.

Smerdon, B. D., C. A. Mendoza, and K. J. Devito (2007), Simulations of fully-coupled lake-groundwater exchange in a sub-humid climate with an integrated hydrologic model, *Water Resour. Res.*, *43*, W01416, doi:10.1029/2006WR005137.

Therrien, R., R. G. McLaren, E. A. Sudicky, and S. M. Panday (2005), HydroGeoSphere v1.13: A three-dimensional numerical model describing fully-integrated subsurface and surface flow and solute transport.

Thornthwaite, C. W. (1948), An approach toward a rational classification of climate, *Geogr. Rev.*, *38*, 55–94.

Winter, T. C. (1986), Effect of groundwater recharge on configuration of the water table beneath sand dunes and on seepage in lakes in the sandhills of Nebraska, U.S.A., *J. Hydrol.*, *86*, 221–237.

K. J. Devito, Department of Biological Sciences, University of Alberta, Z 914/916, Biological Sciences Bldg., Edmonton, AB T6G 2E9, Canada.

C. A. Mendoza and B. D. Smerdon, Department of Earth and Atmospheric Sciences, University of Alberta, 1-26 Earth Sciences Building, Edmonton, AB T6G 2E3, Canada. (brian.smerdon@gmail.com)